

1 BV technique for investigating 1-D interfaces

Nicolas Dorville,¹ Gérard Belmont,¹ Laurence Rezeau,¹ Nicolas Aunai,²

Alessandro Retinò,¹

arXiv:1304.1392v1 [astro-ph.EP] 4 Apr 2013

Corresponding author: N. Dorville, LPP, Ecole Polytechnique, CNRS, UPMC, Université Paris Sud, Palaiseau, France. (nicolas.dorville@lpp.polytechnique.fr)

¹LPP, Ecole Polytechnique, CNRS,
UPMC, Université Paris Sud, Palaiseau,
France

²NASA Goddard Space Flight Center,
NPP - Space Weather Laboratory (674),
Greenbelt, MD, USA

Abstract.

To investigate the internal structure of the magnetopause with spacecraft data, it is crucial to be able to determine its normal direction and to convert the measured time series into spatial profiles. We propose here a new single-spacecraft method, called the BV method, to reach these two objectives. Its name indicates that the method uses a combination of the magnetic field (B) and velocity (V) data. The method is tested on simulation and Cluster data, and a short overview of the possible products is given. We discuss its assumptions and show that it can bring a valuable improvement with respect to previous methods.

1. Introduction

12 The Earth magnetopause is the outer boundary of the terrestrial magnetosphere. Out-
13 side of this boundary, the magnetosheath plasma is the shocked solar wind plasma, *i.e.*
14 cold and dense, with a magnetic field direction essentially determined by the solar wind
15 one. Inside of it, the magnetospheric plasma is comparatively hot and tenuous, with
16 a magnetic field direction essentially determined by the planetary one. Experimentally,
17 investigating the magnetopause structure by spacecraft measurements is made difficult
18 by the fact that the boundary is not steady: it can be shaken by the variations of the
19 solar wind pressure, and perturbed by different kinds of waves, incident body waves as
20 well as surface waves. It can also be locally and temporarily the place of different surface
21 instabilities, implying or not magnetic reconnection, such as Kelvin-Helmholtz, Rayleigh
22 Taylor or tearing instabilities (*Hasegawa et al*, 2012).

23 Two informations are crucial to investigate the magnetopause nature: 1) accurately
24 determine the direction of its normal with respect to the magnetic field (in a strictly
25 stationary configuration, having the normal magnetic field B_n null or not have quite
26 different consequences on the physical nature of the layer, even if the non null B_n is
27 small) and 2) determine an approximate spatial coordinate along the normal, to be able
28 to draw the spatial profiles of the different relevant parameters, in the boundary frame,
29 *i.e* independently of the velocity at which these profiles are traversed by the spacecraft.

30 Several methods have been developed for both of these two purposes.

31 To study the large scale shape of the boundary, its motion and its orientation, multi-
32 spacecraft methods have been developed, particularly for the ESA Cluster mission

33 (*Paschmann and Daly*, 1998 and 2008). These methods are essentially based on tim-
34 ing differences between spacecraft and all rely on strong assumptions on the boundary:
35 its form (plane or slightly curved at the scale of the spacecraft tetrahedron), its station-
36 arity (constant profile and width, hereafter CTA for “Constant Thickness Approach”,
37 (*Haaland et al*, 2004), or its velocity with respect to the spacecraft (hereafter CVA for
38 “Constant Velocity Approach”, *Russell et al* 1983). Others are single spacecraft: they also
39 rely on assumptions on the boundary properties such as planarity and stationarity, but
40 they use in addition theoretical knowledge on the measured physical quantities, such as
41 conservation laws. When using in particular the magnetic field data, the MVAB method
42 (Minimum Variance Analysis on the magnetic field \mathbf{B} , *Sonnerup and Scheible*, 1998) takes
43 advantage that $\text{div}(\mathbf{B}) = 0$, which draws $B_n = cst$ in the 1-D case. Its variant MVABC
44 (C for corrected) adds the constraint $B_n = 0$, using the additional information that the
45 magnetopause normal component B_n is generally close to zero, if not strictly zero. This
46 allows to handle cases when two components are nearly constant and not a single one
47 (*i.e.* when two eigenvalues of the variance-covariance matrix are small). When the mag-
48 netopause can be supposed 1-D and stationary but when its thickness is small, making
49 the kinetic effects non negligible with respect to the MHD ones, the experimental profiles
50 have to be compared with the kinetic models of the tangential layers that can be found in
51 the literature (see *de Keyser and Roth*, 1998, for a review of the first models of this kind,
52 and *Belmont et al.*, 2012, for the most recent one). The experimental method developed
53 in this paper should enable to perform such comparisons. When the magnetopause layer
54 cannot be supposed 1-D, other methods are needed. Some have been developed to recon-
55 struct the magnetopause structure, supposing it is 2-D and stationary, and that it respects

56 MHD equations: these are the Grad-Shafranov reconstruction methods (see *Hasegawa et*
57 *al.*, 2004, for long-duration reconstruction). A review and discussion of short- and long-
58 duration methods is made in *De Keyser* (2006). Experimentally, it is often difficult to
59 decide whether the 1-D or the stationary hypothesis has to be questioned first. Future
60 comparison between the results of the reconstruction methods and those of the method
61 proposed in this paper should be interesting in this respect.

62 To find an approximate normal coordinate allowing to investigate the internal struc-
63 ture of the layer and to determine profiles across it, other methods have been developed
64 independently, introducing the notion of "transition parameter" (*Lockwood and Hapgood,*
65 1997). These methods can be used with single-spacecraft data. They also rely on assumed
66 magnetopause properties, and they have been based hitherto on the variations in density
67 and temperature of the electron population. This of course limits the temporal resolution
68 of the method -and consequently its spatial one- to the electron experiment resolution.

69 We propose here a new single spacecraft method, referred hereafter as "BV" to show
70 that the magnetic field and the flow velocity data are used simultaneously, to analyze
71 magnetopause-like interfaces. It combines the two previous types in such a way that it
72 allows to determine in the same operation the magnetopause normal with an improved
73 accuracy and a transition parameter with an improved time resolution and expectingly
74 closer to a real spatial coordinate. Fitting the magnetic field hodogram with a prescribed
75 form, which is here an elliptical arc, allows to determine the normal direction with a fairly
76 good accuracy. In addition, the angle α characterizing the position on the elliptical arc
77 provides a reliable transition parameter inside the current layer, which can be viewed
78 as a proxy for a normalized coordinate in the normal direction. On the other hand, as

soon as the normal direction is known, the velocity measurements give a non-normalized normal coordinate, which is just the integral of the normal flow velocity u_n . It can give, in particular, a fairly good estimate of the physical width of the layer whenever the measured velocity should be in most cases dominated by the motion of the boundary. Using simultaneously the magnetic and velocity measurements just consists in imposing that the normal coordinate determined by the only velocity measurements is proportional to the transition parameter coming from the only magnetic measurements. Since the integral of u_n is very sensitive to the normal direction, this enables to improve the determination of this direction with respect to the only magnetic one, while the time resolution of $y(t)$ remains approximately the magnetic one, which is much better than the velocity resolution.

Section 2 presents the principles of the BV technique, and section 3 the different validation tests performed. The method allows to draw spatial profiles of any physical parameter across the magnetopause boundary. Examples of such profiles are presented in section 4, before discussing the interest and the limitations of the BV method and concluding in section 5.

2. Principles of the method

As the previous equivalent methods, the basic assumption of the BV technique is that, apart from oscillating perturbations, the boundary is sufficiently one dimensional and stationary at the scale of the spacecraft crossing. To explain the principles of this method, we use here a set of Cluster data on March, 3rd, 2008, when Cluster C3 encounters the magnetopause around 23:16, as it can be seen on Fig. 1 from the transition in the energy composition of the plasma, the density gradient and the rotation of magnetic field

101 observed. The method uses principally the magnetic field data (*Balogh et al.*, 1997). In
102 subsection 2.1 we describe how we obtain an initial guess with only magnetic field data.
103 Subsection 2.2 then explains the BV method itself, which combines magnetic field and
104 ion velocity data.

2.1. Initialization with the only magnetic field data

105 In order to correctly initialize the minimization process of the complete BV method,
106 involving magnetic field and ion velocity data, it is necessary to perform first an initializa-
107 tion stage, which provides an approximated frame and a first elliptical fit. This stage uses
108 only the magnetic field data. It is done itself in several steps. The first step consists in
109 finding a first approximation of the normal direction via a MVABC technique (*Sonnerup*
110 *and Scheible*, 1998). Fig. (2) shows the tangential hodogram derived by this method. In
111 this example as in many other observations (*Panov et al.*, 2011), we observe a C-shaped
112 hodogram, which can be fitted by an elliptical model. Although the general concept of
113 the BV method is valid for any 1D layer, its present implementation is conceived for such
114 kind of hodograms. Further generalization to more complicated hodograms (in particular
115 for the S-shaped hodograms described in *Panov et al.*, 2011) is of course always possible.
116 The second step consists in selecting the “magnetic ramp”, *i.e.* the interval of data where
117 the gradient of B_L is located. We then further select the data points by choosing only
118 a sample of “representative points” among them. This step has a double purpose: elim-
119 inate the perturbations that can be considered as “noise”, and make the different parts
120 of the crossing equally represented in the statistics, even if the spacecraft does not spend
121 the same time in these different parts. First we roughly eliminate the perturbations by
122 discarding all points too far from the mean trajectory of the hodogram, and we represent

123 each too close packet of points by only one single point. An elliptic fit and a new reference
 124 frame are derived from these points, using a Powell algorithm. The points selected in this
 125 way and the correspondent fit in the new frame are shown in Fig. (3). Then, the second
 126 goal is achieved by keeping a constant number of points in each α slice, which corresponds
 127 to the hypothesis (to be justified in next section) that α varies linearly with y . A new
 128 elliptic fit and approximated frame are then obtained, which provides a fine initialization
 129 for the BV method itself.

2.2. Simultaneous use of magnetic and velocity data

The above stage has given an initial guess for the BV method regarding 1) the normal direction, and 2) the parameters describing the elliptic hodogram. The main part of the method then consists in using the temporal information $\mathbf{B}(t)$, together with the velocity measurements from the Hot ion analyser experiment (*Rème et al, 1997*). Going back to the totality of the \mathbf{B} data points, one minimizes the distance between them and the elliptical model $\mathbf{B}(y)$, the function $y(t)$ being the integral of the normal velocity u_n . We therefore assume that this velocity is dominated by the layer velocity, *i.e.* that the normal velocity in the layer frame is zero or negligible. The minimization is done with respect to the three angles that characterize the rotation of the ellipse proper frame and to the parameters of the elliptic hodogram, initialized previously, using the same Powell algorithm as above. The distance to be minimized is:

$$\sum \sqrt{(B_{dx} - B_{mx})^2 + (B_{dy} - B_{my})^2 + (B_{dz} - B_{mz})^2} \quad (1)$$

130 Where \mathbf{B}_d represents the data points and \mathbf{B}_m represents the model. This model is given
 131 by:

$$B_{mx} = B_{x0} \cos \alpha \quad (2)$$

$$B_{my} = B_{y0} \quad (3)$$

$$B_{mz} = B_{z0} \sin \alpha \quad (4)$$

with:

$$\alpha = \alpha_1 + (\alpha_2 - \alpha_1) y/y_{max}, \quad (5)$$

132 y being the position deduced from the normal velocity integral. The magnetic field data
 133 and velocity data are obtained from prepared data by a rotation of $M(\theta, \phi, \chi)$. The
 134 parameters of the fit are $\theta, \phi, \chi, B_{x0}, B_{y0}, B_{z0}, \alpha_1$, and α_2 .

135 This final stage provides all the needed outputs: the normal direction, the spatial
 136 position $y(t)$ along this normal (measured directly in physical units, providing in particular
 137 the layer thickness in km), and the fit of magnetic field, as illustrated, for example, on
 138 Fig. (4). Here the computed magnetopause thickness is 1800 km and the linear Pearson
 139 correlation coefficients of the fit of B_x and B_z are 0.99 and 0.95. The spatial position y
 140 is then extrapolated linearly outside the boundary, in order to plot approximated profiles
 141 of any plasma parameter on scales larger than the ramp region if necessary.

3. Validations of the method

142 Having presented how the BV method works in the previous section, we will now explain
 143 what led us to this way of proceeding and what are the different validation tests we have
 144 performed. We will discuss first the validity and the limitations of the hypotheses done,
 145 and discuss afterward the consistency of the obtained results. We used three different

146 tools to develop and validate the method: - a simple code to generate artificial magnetic
 147 field data, - a hybrid simulation of an asymmetric reconnection layer (*Aunai et al*, 2013b),
 148 - and real data from the Cluster mission, especially a 2008 low latitude crossings list
 149 compiled by N. Cornilleau-Wehrin.

3.1. Hypotheses: elliptical shape and linear angular velocity

150 The first new assumption of the method, with respect to previous single spacecraft data
 151 analysis methods, is the elliptic shape of the tangential magnetic field hodogram, the
 152 simplest model geometry to describe C-shaped hodograms. This elliptical shape is indeed
 153 consistent with a simple generalization of the circular model $\mathbf{B}(y)$ proposed by (*Panov et*
 154 *al*, 2011):

$$\frac{B_L}{B_{L0}} = \tanh(y/L) \tag{6}$$

$$\frac{B_M}{B_{M0}} = \frac{1}{\cosh(y/L)} \tag{7}$$

155 These formulas imply in particular that $B_L^2/B_{L0}^2 + B_M^2/B_{M0}^2 = 1$, which can be a test of
 156 the elliptical shape.

157 The efficiency of the method can be tested first on a numerical simulation of reconec-
 158 tion (*Aunai et al*, 2013b), far from the X point. Its applicability is not obvious in this case,
 159 since, before the development of the reconnection pattern, the initial condition is purely
 160 tangential, without any rotation. Nevertheless, the Hall effect creates a self-consistent
 161 out-of-plane magnetic component during the reconnection process, which, in the consid-
 162 ered asymmetric configuration (asymmetric in density and temperature and coplanar and
 163 antisymmetric in magnetic field), results in a C-shaped hodogram if looked between the
 164 separatrices. Fig. (5) shows the magnetic field in the interval that corresponds to the

165 gradient of B_L . The error is here less than 2 percent. We have checked that this good
166 accuracy is kept as long as the crossing considered is not too close to the X-point, which
167 is generally the case for crossings of reconnected magnetopause or to the limits of the
168 simulation.

169 Concerning the analytical form of $\alpha(y)$, we also checked the validity of the linear hy-
170 pothesis in the same simulation study. Fig. (6) shows how α varies as a function of
171 the normal coordinate y_s of the simulation. We observe that, apart from weak periodic
172 variations, the linear form is well satisfied. It is worth explaining that the weak periodic
173 departures from the linear variations (which can be well described by the three or four first
174 terms of a Fourier transform) can indeed be accounted for in the minimization procedure,
175 but it would increase the number of free parameters and drastically affect the convergence
176 of the minimization process.

3.2. Consistency of the results and limitations

177 Regarding the consistency of the results, the first test consists in running the first part
178 of the method (identification of the ellipse and of its proper frame) on a magnetic field
179 that is artificially generated with an elliptic hodogram. Such artificial data have thus
180 been constructed with the same analytical formulas as those of the program, then turned
181 on a random frame, and added with a random Gaussian noise centered on the signal,
182 with a relative amplitude up to 50%. The result is that the method always allows to find
183 the good initial normal direction with at least 5 significant numbers, as well as the right
184 ellipse parameters, whenever the noise does not exceed 30%.

185 The second test consists in using the above numerical simulation (*Aunai et al, 2013b*) to
186 mimic a real magnetopause crossing. In order to make the method work, we must modify

187 the simulation results in a way that makes it likely closer to most real magnetopause
 188 crossing: we multiply the tangential velocities by a large factor (≈ 10). Thanks to this
 189 change, the tangential velocities get a much larger contrast than the normal ones, which
 190 is necessary for the program convergence. It must be noted that such a contrast of
 191 the tangential velocities does generally exist at the magnetopause, since the tangential
 192 velocity change is generally of the order of a few 100 km/s, while the normal one (in
 193 the spacecraft frame) is generally about ten times smaller and varies very little. In order
 194 to focus on the reconnection process freely of any KH instability, the simulation did not
 195 include such a velocity shear. Furthermore, the normal velocity of the virtual spacecraft
 196 considered with respect to the boundary, has to be chosen large enough with respect to the
 197 normal velocities in the boundary frame. This is also, as already mentioned, a reasonable
 198 hypothesis for a real magnetopause crossing.

199 Under these assumptions, we get normals with an angular precision oscillating between
 200 0 and 5 degrees (with the corresponding errors on the shape of the tangential hodogram)
 201 and 0-5% errors on the y parameter (and derivative), which corresponds to the internal
 202 velocity and the approximations on $\alpha(y)$.

203 The result is not changing as long as the virtual spacecraft crosses the simulation far
 204 enough (several d_i) from the X point, where the 2D effects are not dominant. In these
 205 cases, the precision of the MVABC method is of the same order, (slightly better or worse,
 206 depending on the cases), because B_n is actually very close to 0.

207 Regarding real Cluster data, the measurements show more perturbations, but the varia-
 208 tions of the field value around the mean ellipse are still around 5 percent for most C-shaped
 209 hodograms. A good test for the elliptical shape is to plot $B_z^2(B_x^2)$, that should be linear

210 for a tangential ellipse. Fig. (7) shows this plot for two magnetopause crossings on
211 03/03/2008 and 04/01/2008. It shows that the elliptical shape is a good approximation.

212 It is clear, from the the tests on the numerical simulation, that the BV method has
213 limitations related to the necessary contrast between the normal and tangential component
214 profiles. When applied to real Cluster data, these limitations may have, in some occasions,
215 consequences on the results obtained. We will discuss these limitations in the conclusion
216 section. It is to be noted however that these limitations are based on assumptions which
217 are different -and generally weaker- than those of the other single-spacecraft methods such
218 as MVAB or MVABC.

219 We will present a detailed study on a case (*Dorville et al, 2013*), where the BV method
220 leads to a better understanding and more precise results than MVAB(C). When all the
221 methods are confidently applicable, the results seem to be consistent with each other and
222 with the theoretical knowledge. We show on Fig. (8) "oeil" a reproduction of a figure from
223 (*Haaland et al, 2004*) corresponding to a benchmark case where different methods have
224 been used. The center of the figure is the mean MVABC normal and other single and
225 multi-spacecraft methods are represented in a polar plot in the plane perpendicular to this
226 normal. The result of the BV method on C1 spacecraft is indicated by a star. The figure
227 shows that, if the result is different from other methods, it is inside the dispersion range of
228 the points. The thickness of the layer always stands between a few hundreds of kilometers
229 and a few thousands, which is consistent with literature, the tangential velocities being
230 generally one order of magnitude larger than the normal one (in the spacecraft frame).
231 The normal magnetic fields always stand between 0 and 20 nT, the non null values being

232 reliable and quantitative indications of a connected boundary, which could hardly be
233 obtained previously.

4. Products of the method

234 As explained above, the first main direct product of the method is an accurate deter-
235 mination of the direction normal to the boundary, leading to reliable values of the small
236 components B_n and u_n of the magnetic field and the flow velocity across the boundary.
237 The second direct product is the determination of a spatial coordinate $y(t)$ allowing to
238 draw any plasma parameter profile against the spatial position y from their temporal mea-
239 surement. The magnetopause layer thickness is also an interesting by-product deriving
240 directly from the two preceding ones.

241 Examples of y profiles are presented in Fig. (9) for the crossing of 03/03/08. Here we
242 see the characteristic jump of density at the magnetopause, but no temperature jump,
243 the pressure evolving like the density. For the different crossings that we investigated,
244 we could often observe clear differences concerning the locations of the particle gradients
245 with respect to the magnetic field rotation. In a companion paper, we will present an
246 interesting case study where the BV method can bring new information about the nature
247 of the magnetopause.

248 In Fig. (10) the normal electric field obtained with the EFW experiment (*Gustafsson et*
249 *al.*,(2001)) and the tangential components are shown for the same 03/03/2008 crossing. We
250 see that the maximum variance is on the normal electric field, as expected by theory, and
251 quite constant tangential electric fields, which confirms that the normal direction found
252 is a good one. Fig. (11) shows the profiles of magnetic field spectral power density ob-
253 tained with the STAFF experiment (*Cornilleau-Wehrlin et al.*, 2003) for different frequency

254 ranges. One can observe that the source of waves lies in the magnetosheath and that the
255 depth of penetration depends on the frequency, the lowest frequencies penetrating deeper
256 toward the magnetospheric side.

257 This ability to get spatial profiles of all the quantities in the boundary is a key to a
258 better understanding of the physical nature of the magnetopause.

5. Discussion and conclusion

259 We have presented the new BV method to analyze the structure of the magnetopause
260 boundary layer, using spacecraft data. It combines the magnetic field and velocity mea-
261 surements of one single spacecraft and permits to find the normal direction and a good
262 resolution on a spatial coordinate to resolve small scale variations inside the layer. Using
263 it, we are able to study the internal structure of the layer, for any of the physical quan-
264 tities measured on board. The method works on simulation and generated data, and its
265 assumptions can be verified on Cluster crossings.

266 It is worth observing the conditions of validity of the BV method are not the same
267 as the other single spacecraft methods such as MVAB, and that they are in general less
268 restrictive. In MVAB, one needs to discriminate B_N and B_M , which fails systematically in
269 structures as shocks, and often at the magnetopause since this one is often quasi-coplanar.
270 MVABC has the same condition of validity, with the additional problem that it cannot
271 be used for determining B_n since this component is supposed null. In the BV method,
272 one needs to discriminate the two couples of data sets: (B_N, V_N) and (B_M, V_M) . This is
273 clearly a weaker condition since, even if B_N and B_M are nearly constant, the differences
274 between V_N and V_M , (profiles and/or orders of magnitude) are generally sufficient to

275 guarantee a correct operation. The difficulties can only arise when not only B_N and B_M
276 are indistinguishable (mean jump much smaller than noise), but also V_N and V_M .

277 Contrary to the multi-spacecraft timing methods, the BV method can also handle cases
278 when the boundary is shaken with a non trivial normal velocity evolution (which seems
279 frequent). When this evolution is non negligible between two spacecraft crossings, the
280 timing methods obviously fail.

281 The BV method however brings a new limitation: although one works essentially with
282 magnetic field data, a sufficiently long crossing is needed (at least three or four velocity
283 measurement points inside the crossing) to make efficient the contribution of the velocity
284 data. We are therefore not able to analyze as many crossings as the other methods.

285 With the proposed method, the structure of the magnetopause should be now open to
286 more detailed investigations. Some examples of spatial profiles have been given in section
287 4. The method is used in a companion article, for an atypical magnetopause case study
288 giving new insight on this structure.

289 **Acknowledgments.** The authors would like to thank N Cornilleau-Wehrin for fruitful dis-
290 cussion and her help to work with Cluster data and detect magnetopause crossings, and the CAA
291 and all Cluster instruments teams for their work on Cluster data.

References

292 Aunai, N., G. Belmont, and R. Smets (2011), Proton acceleration in antiparallel collisionless
293 magnetic reconnection: Kinetic mechanisms behind the fluid dynamics, *J. Geophys. Res.*, 116,
294 A09232, doi:10.1029/2011JA016688.

- 295 Aunai, N., et al. Comparison between hybrid and fully kinetic models of asymmetric magnetic
296 reconnection: Coplanar and guide field configurations. *Physics of Plasmas* 2013; 20: 022902.
- 297 Balogh, A., Dunlop, M. W., Cowley, S. W. H., Southwood, D. J., Thomlinson, J. G., and the
298 Cluster magnetometer team: The Cluster magnetic field investigation, *Space Sci. Rev.*, 79, 65,
299 1997
- 300 Cornilleau-Wehrin, N., Chanteur, G., Perraut, S., Rezeau, L., Robert, P., Roux, A., de Villedary,
301 C., Canu, P., Maksimovic, M., de Conchy, Y., Hubert, D., Lacombe, C., Lefeuvre, F., Parrot,
302 M., Pinon, J. L., Dcrau, P. M. E., Harvey, C. C., Louarn, Ph., Santolik, O., Alleyne, H. St. C.,
303 Roth, M., Chust, T., Le Contel, O., and STAFF team: First results obtained by the Cluster
304 STAFF experiment, *Ann. Geophys.*, 21, 437-456, doi:10.5194/angeo-21-437-2003, 2003.
- 305 De Keyser, J. (2006), The Earth magnetopause: reconstruction of motion and structure, *Space*
306 *Science Reviews* 121: 225-235
- 307 De Keyser, J., and M. Roth (1998), Equilibrium conditions and magnetic field rota-
308 tion at the tangential discontinuity magnetopause, *J. Geophys. Res.*, 103(A4), 66536662,
309 doi:10.1029/97JA03710.
- 310 Dorville N., G.Belmont, L. Rezeau, R. Grappin, A. Retino, Rotational/ Compressional nature of
311 the Magnetopause: Application of the BV technique on a magnetopause case study, submitted
312 to JGR, 2013
- 313 Gustafsson, G., Andr, M., Carozzi, T., Eriksson, A. I., Flthammar, C.-G., Grard, R., Holm-
314 gren, G., Holtet, J. A., Ivchenko, N., Karlsson, T., Khotyaintsev, Y., Klimov, S., Laakso, H.,
315 Lindqvist, P.-A., Lybekk, B., Marklund, G., Mozer, F., Mursula, K., Pedersen, A., Popielawska,
316 B., Savin, S., Stasiewicz, K., Tanskanen, P., Vaivads, A., and Wahlund, J.-E.: First results of
317 electric field and density observations by Cluster EFW based on initial months of operation,

- 318 Ann. Geophys., 19, 1219-1240, doi:10.5194/angeo-19-1219-2001, 2001.
- 319 Haaland, S., Sonnerup, B., Dunlop, M., Balogh, A., Georgescu, E., Hasegawa, H., Klecker, B.,
320 Paschmann, G., Puhl-Quinn, P., Rème, H., Vaith, H., and Vaivads, A., 2004a, Four-spacecraft
321 determination of magnetopause orientation, motion and thickness: comparison with results
322 from single-spacecraft methods, Ann. Geophys., 22, 1347-1365
- 323 Hasegawa, H. (2012), Structure and dynamics of the magnetopause and its boundary layers,
324 Monogr. Environ. Earth Planets, 1, 71-119, doi:10.5047/meep.2012.00102.0071.
- 325 Hasegawa, H. et al (2004), Reconstruction of two-dimensional magnetopause structures from Clus-
326 ter observations: verification of method, Annales Geophysicae (2004) 22: 1251-1266.
- 327 Lockwood, M., and M. A. Hapgood, How the magnetopause transition parameter works, Geo-
328 phys. Res. Lett., 24, 373-376, 1997.
- 329 Panov, E. V., A. V. Artemyev, R. Nakamura, and W. Baumjohann (2011), Two types of tan-
330 gential magnetopause current sheets: Cluster observations and theory, J. Geophys. Res., 116,
331 A12204, doi:10.1029/2011JA016860.
- 332 Paschmann, G., and Daly, P. W., 1998, Analysis Methods for Multi-spacecraft data, no. SR-001
333 in ISSI Scientific Reports, ESA Publ. Div., Noordwijk, Netherlands.
- 334 Paschmann, G., and Sonnerup, B. U. ., 2008, Proper Frame Determination and Waln Test, in
335 Multi-spacecraft Analysis Methods Revisited, edited by G. Paschmann and P. W. Daly, no.
336 SR-008 in ISSI Scientific Reports, ESA Publ. Div., Noordwijk, Netherlands.
- 337 Rème, H., Cottin, F., Cros, A., et al.: The Cluster Ion Spectrometry (CIS) Experiment, Space
338 Sciences Review 79, 303-350, 1997
- 339 Russell, C. T., Mellot, M. M., Smith, E. J., and King, J. H., 1983, Multiple spacecraft observations
340 of interplanetary shocks: Four spacecraft determination of shock normals, J. Geophys. Res., 88,

341 47394748.

342 Sonnerup, B. U. ., and Scheible, M., 1998, Minimum and Maximum Variance Analysis, in Analysis
 343 Methods for Multispacecraft Data, edited by G. Paschmann and P. W. Daly, no. SR-001 in
 344 ISSI Scientific Reports, chap. 8, pp. 187-196, ESA Publ. Div., Noordwijk, Netherlands.

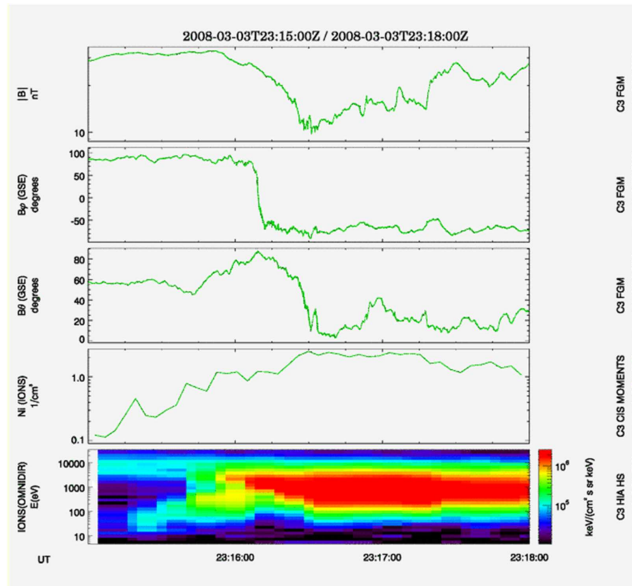


Figure 1. Density, energy spectrogram and magnetic field observed by Cluster C1 around 23h16 on 03/03/2008. The jump of density, change in plasma energy composition and rotation of magnetic field show that the satellite is crossing the magnetopause.

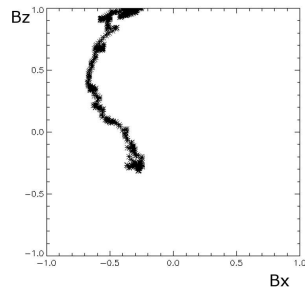


Figure 2. Hodogram of the magnetic field in the tangential MVABC plane for the Cluster C3 magnetopause crossing of 03/03/2008.

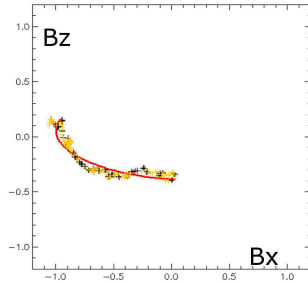


Figure 3. Initialization fit of the hodogram in initialization frame for the Cluster C3 magnetopause crossing of 03/03/2008. The data is in black, the selected points in yellow and the initialization fit in red.

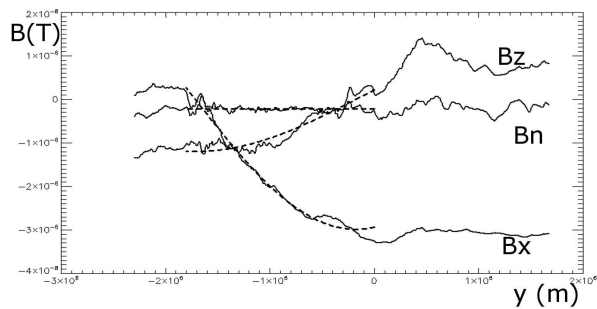


Figure 4. Fit (dashed) of the three components of the magnetic field (solid lines) along the normal coordinate for the Cluster C3 magnetopause crossing of 03/03/2008.

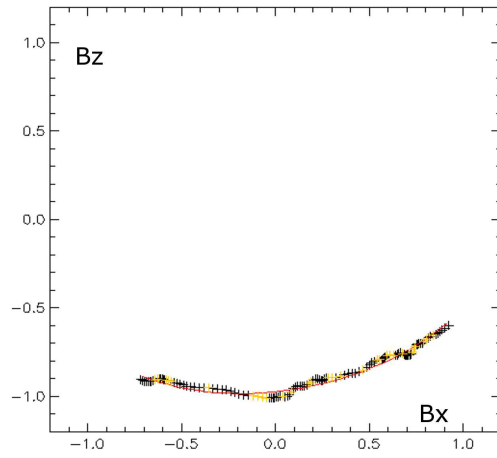


Figure 5. Fit of the hodogram of the magnetic field in the simulation for a virtual satellite crossing far from X point in the numerical simulation. The data is in black, the selected points in yellow and the fit in red.

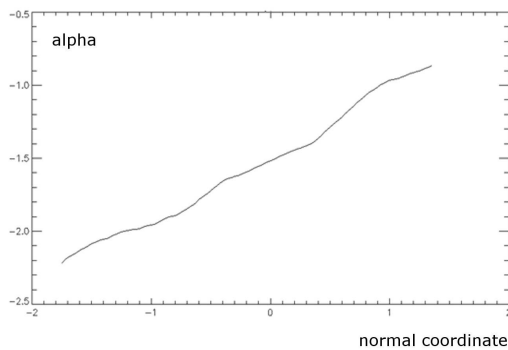


Figure 6. Angular position on the ellipse along the normal direction in the simulation for a virtual satellite crossing far from X point.

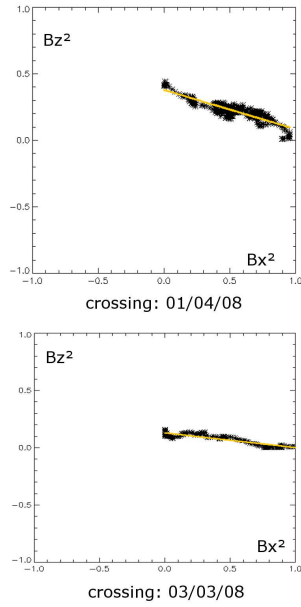


Figure 7. Hodogram of the squared components of magnetic field in the LM plane for two Cluster C3 magnetopause crossings of April, 1st 2008 and March, 3rd, 2008.

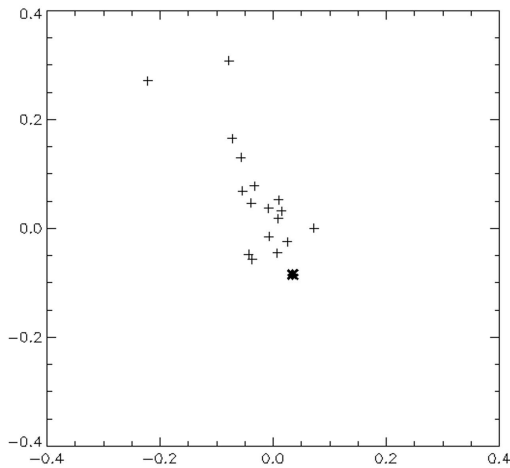


Figure 8. Several single and multi-spacecraft methods normal direction positions in the plane perpendicular to the MVABC mean normal for a benchmark case from (*Haaland et al, 2004*). The star represents the result of BV method. The distance from the origin in this plane corresponds to the $\sin \theta$, where θ is the angle from the mean normal direction.

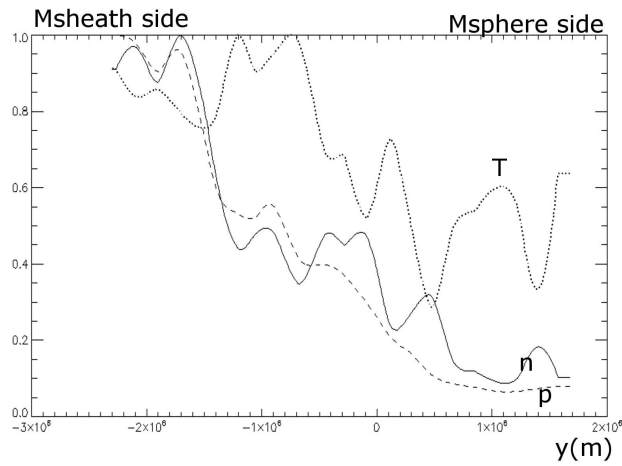


Figure 9. Evolution with normal position of density, pressure and temperature measured by Cluster C3 for the 03/03/2008 crossing.

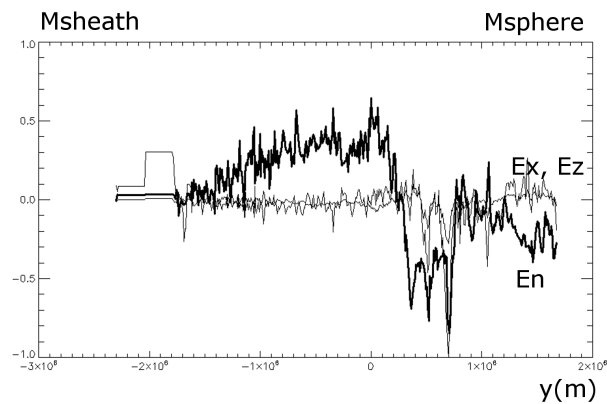


Figure 10. Evolution with normal position of the Electric field measured by Cluster C3 for the 03/03/2008 crossing.

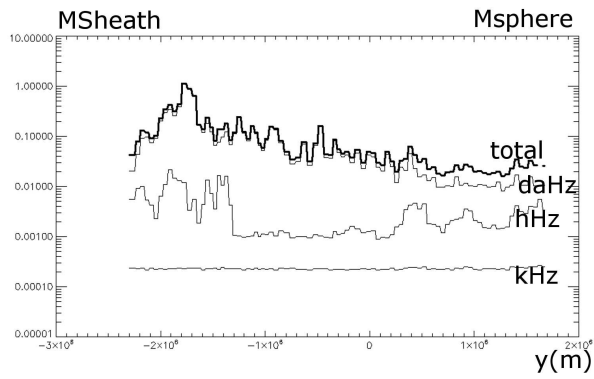


Figure 11. Evolution with normal position of the spectral power density for magnetic field measured by Cluster C3. The total spectral power density is the thick line, as the daHz hHz and kHz frequency ranges are also represented on the same scale.